

# Multi-aquifer susceptibility analyses for supporting groundwater management in urban areas

Licia C. Pollicino<sup>1,2</sup>, Marco Masetti<sup>1</sup>, Stefania Stevenazzi<sup>1</sup>, Agata Cristaldi<sup>3</sup>, Chiara Righetti<sup>3</sup>, Maurizio Gorla<sup>3</sup>

<sup>1</sup>Dipartimento di Scienze della Terra “A. Desio”, Università degli Studi di Milano, 20133 Milan Italy;

<sup>2</sup>Dipartimento di Ingegneria Civile e Ambientale (DICA), Politecnico di Milano, 20133 Milan, Italy;

<sup>3</sup>Gruppo CAP, Ufficio Progetto PIA e Bonifiche - Direzione Ricerca e Sviluppo, Milan, Italy.

## Highlights

Multi-source diffuse pollution seriously threatens water quality in the Milan area

Shallow and deep aquifers susceptibility to PCE+TCE and Cr(VI) pollution is mapped

The effect of hydrogeological and land use factors is quantified at a regional scale

The influence of aquitard heterogeneities and multi-aquifer wells is investigated

## Abstract

In the densely urbanised Milan Metropolitan area (northern Italy), the long history of anthropogenic activities still exerts a significant pressure on groundwater resource. One of the most serious threats to the water quality of urban aquifers is attributed to diffuse contamination, which is caused by a series of unknown small sources (i.e., multiple point sources) distributed over large areas. In the study area and in many industrialised regions of the world, tetrachloroethylene [PCE], trichloroethylene [TCE] and hexavalent chromium [Cr(VI)] represent the common example of long-standing and persistent pollution in groundwater. In the Milan Metropolitan area, high levels of PCE+TCE and Cr(VI) were detected in the shallow aquifer as well as in the deep aquifer.

To assess and map the shallow and deep aquifers susceptibility to PCE+TCE and Cr(VI) contamination at a regional scale, the Weights of Evidence modelling technique has been applied. This method has been used to objectively evaluate the spatial correlation between the high presence of these pollutants in each aquifer and hydrogeological and land use factors that can potentially influence the contamination. Moreover, the results allowed us to quantify on a large scale the effect that preferential flowpaths, due to both thickness variation in the aquitard and the areal density of multi aquifer wells, have in reducing the protection of the underlying deep aquifer. The end-products of the study constitute

a key tool to be used by water-resource managers and decision-makers for the improvement of groundwater management and protection strategies.

## **Keywords**

chlorinated solvents, hexavalent chromium, diffuse contamination, spatial statistical method, Milan.

## **1 Introduction**

More than half of the world's population lives in urban areas and it is estimated that most of the population increase in the next decades will find accommodation in urban areas (UNPD, 2018). Urban growth significantly affects the availability of groundwater resource through increasing demand for safe drinking water supplies (WWAP, 2012). Additionally, the progressive extension of urbanised areas leads to the development of point, non-point and multiple-point sources of contamination that can seriously deteriorate groundwater quality. One of the most common solutions to provide safe drinking water consists in pumping groundwater from a more protected deep aquifer. Nevertheless, the intensive exploitation of deep aquifers can contribute to increase their susceptibility by creating preferential flow paths from the contaminated shallow aquifer to the deepest ones (Johnson et al., 2011; Eberts et al., 2013).

Currently, among the different categories of contamination sources (i.e., point sources, non-point sources, multiple-point sources), multiple-point sources represent one of the most serious threats to the quality of urban groundwater as they are responsible for diffuse contamination. Over time, plumes may mix with each other and end into a diffuse pattern of pollution linked to unidentifiable multiple-point sources, which, in most cases, started decades ago (Cortés et al., 2011). These multiple-point sources are difficult to detect since they are distributed over large areas and release a small contaminant mass (Alberti et al., 2018). Therefore, groundwater diffuse contamination cannot be remediated by adopting the traditional remediation techniques and this reinforces the urgent need to invest economically in finding new and alternative solutions.

In addressing this environmental issue, the cooperation between water resources managers and the scientific community can play a major role in developing scientifically-based actions to prevent the formation of new diffuse contaminated areas and support safe and cost-efficient management of the

existing ones. To set up and test new approaches to enhance groundwater protection, the Milan Metropolitan area (northern Italy) can be adopted as a pilot case study. In the Milan Metropolitan area, both shallow and deep aquifers are characterised by the presence of chlorinated solvents (i.e., tetrachloroethylene [PCE], trichloroethylene [TCE]) and hexavalent chromium [Cr(VI)] that represent an example of long-standing and widespread pollution common in many parts of Italy and the world (Izbicki et al., 2008; Rivett et al., 2012; Nijenhuis et al., 2013; Tiwari et al., 2019).

Both chlorinated solvents and Cr(VI) contamination in groundwater have been detected since the 1960s, mainly due to the rapid growth of industrial and commercial activities at the end of World War II (Giovanardi, 1979; Cavallaro et al., 1985; Segre, 1987; Provincia di Milano, 1992; Berbenni et al., 1993). Although these sources of contamination have been progressively dismantled and/or reclaimed, both PCE+TCE and Cr(VI) still occur as solutes in groundwater in both shallow and deep aquifers showing concentration levels above the drinking water limit over large areas (i.e., as diffuse contamination; Pedretti et al., 2013; Azzellino et al., 2019, Colombo et al., 2019). The occurrence of these contaminants in both aquifers is also facilitated by the fact that human infrastructures can interfere with the hydrogeological system and alter the mutual interaction between the aquifers (e.g., multi-aquifer wells, underground pipes) causing a potential cross-contamination between the aquifers (Santi et al., 2006).

An extremely useful tool to derive key information for water protection is represented by groundwater vulnerability maps. As described by several authors (e.g., Focazio et al., 2002; Stumpp et al., 2016; Wachniew et al., 2016), the approaches used to determine aquifer vulnerability can be categorised in subjective (e.g., DRASTIC, Aller et al., 1987; GOD, Foster, 1987; SINTACS, Civita et al., 1994) and objective methods (e.g., Logistic Regression, Tesoriero and Voss, 1997; Winkel et al., 2008; Conditional probability (i.e., Bayesian), Arthur et al., 2007; Non-linear regression models, Nolan and Hitt, 2006; Fuzzy logic, Artificial Neural Network, Gemitzi et al., 2006; process-based methods, Eberts et al., 2012; Beaujean et al., 2014). For the subjective methods, the importance of each parameter in controlling groundwater vulnerability depends on the judgement and expertise of the hydrogeologist. Conversely, the objective methods include statistical approaches for the evaluation of the relationship between the predictor factors and groundwater contamination. In this case, the role of each factor in

influencing groundwater vulnerability is independent of expert-opinion and the final product is more scientifically defensible.

Among the various groundwater vulnerability assessment approaches, we selected the Weights of Evidence technique (WofE; Bonham-Carter, 1994) as the most appropriate to cope with the groundwater diffuse pollution problem at a regional scale. The WofE approach has been widely used both in geosciences including mineral exploration (Agterberg et al. 1993; Raines and Mihalasky, 2002) and landslide hazard zonation (Lee et al., 2002; Poli and Sterlacchini, 2007) and in many other fields, such as archaeology (Duke and Steele, 2010), ecology (Romero-Calcerrada and Luque, 2006) and epidemiology (Lynen et al., 2007). Applications in groundwater vulnerability assessment have mainly focused on the quality deterioration of the unconfined shallow aquifer due to non-point sources contamination at a regional scale (e.g., Arthur et al., 2007; Uhan et al., 2011; Stevenazzi et al., 2015). As in most groundwater vulnerability analyses, these works investigate the effect that hydrogeological factors have on the fate and transport of the contaminant into the aquifers (i.e., groundwater flow velocity, groundwater table depth, hydraulic conductivity of the vadose zone). In addition, these studies take into account factors potentially responsible for contaminant release from the surface (e.g., contaminant loads).

In absence of a standardised and unanimously accepted definition of the concept of groundwater vulnerability in hydrogeology (Liggett and Talwar, 2009; Wachniew et al., 2016), we prefer to adopt the term “susceptibility” as a synonym for “vulnerability” to indicate the sensitivity of an aquifer to being adversely affected by a contaminant load coming from the surface (Foster et al., 2013)

In this study, we investigate: i) the combination of natural and anthropogenic factors influencing PCE+TCE and Cr(VI) contamination in groundwater and ii) the impact that the most “exposed” shallow aquifer could have on groundwater deterioration in the less “exposed” deep aquifer. The study takes advantage of the European Community guidelines that uses a dedicated monitoring network based on water safety plan actions to ensure the availability of a great amount of hydrochemical data.

The main objective of this study is to explore some key issues for managing diffuse contamination in groundwater resources over large areas, such as: a) determining the role that potential sources of

contamination can have on groundwater quality, considering that sources can be different in type and size depending on the aquifer of interest (unconfined, confined); b) identifying the areas that are more susceptible to the presence of groundwater diffuse contamination; and c) deriving quantitative information to guide the measures for aquifer protection from contamination at a regional scale.

## **2 Study area**

The study area is located in the Lombardy Region within the Po Plain in northern Italy and covers an area of about 2000 km<sup>2</sup>, corresponding to the Metropolitan area of Milan (Fig. 1), where residential and commercial buildings, as well as industrial and agricultural activities are present. The elevation ranges between 80 and 250 m a.s.l.. The area is bounded by the Prealps foothills along the north and by the Adda and Ticino rivers to the east and west, respectively. The hydrographic system of the Po Plain includes the Ticino and Adda rivers, flowing from Lake Maggiore and Lake Como, respectively, to the Po River. Olona, Seveso and Lambro rivers flow within the investigated area. Moreover, the study area is characterised by a complex irrigation waterway network: the Villoresi canal flows from the east to the west, from the Ticino River towards the Adda River, and the Muzza canal flows in the eastern sector, as a branch of the Adda River. The Naviglio Grande-Naviglio Pavese waterways flow in the western sector of the study area, from the Ticino River to the city of Milan (Naviglio Grande) and from Milan towards the Ticino River. These canals feed a fully gravity-driven irrigation network by means of secondary and tertiary waterways.

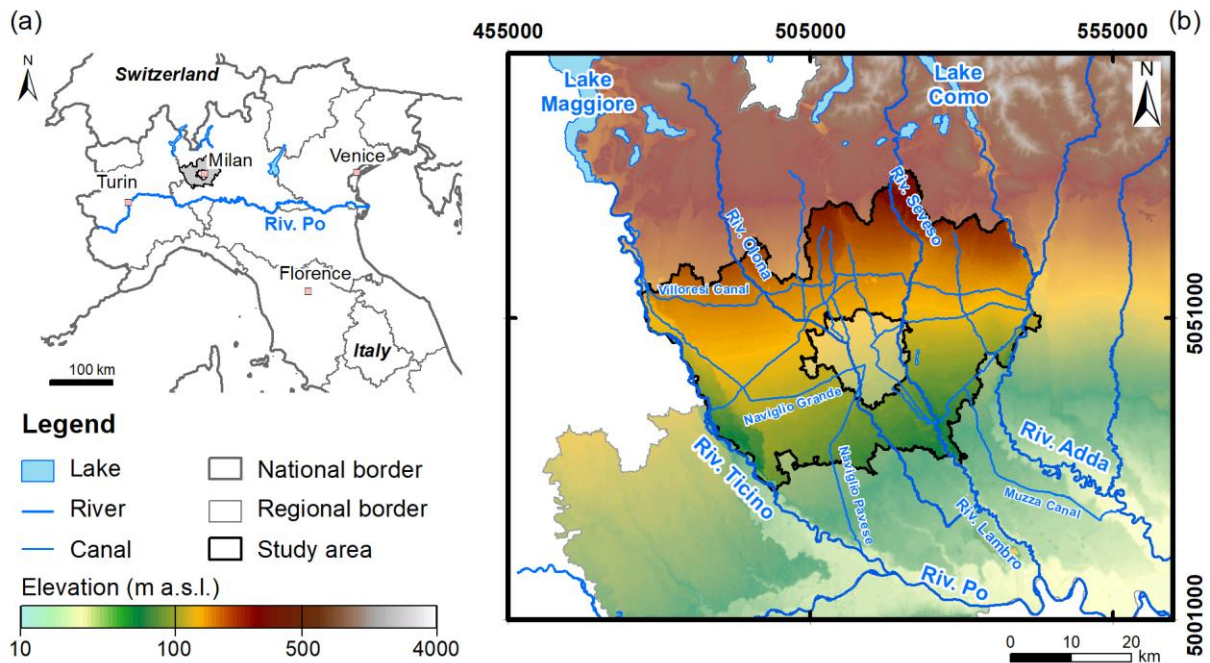


Fig. 1 – a) Location of the study area (in grey); b) Study area and hydrographic system (main rivers, main canals and lakes).

The Po Plain aquifer system consists of four main aquifers, called Aquifers Groups (Regione Lombardia and ENI Divisione Agip, 2001; Gorla, 2001a; Gorla 2001b): A, B, C and D, from the top to the bottom of the sequence, respectively (Fig. 2). The deepest aquifer, Aquifer Group D, is not considered in this study. The shallow unconfined aquifer (Aquifer Group A) is characterised by a coarse lithology, mainly gravel with a sandy matrix of high-energy fluvial environments, with origins generally from north to south, dated as Middle-to-Late Pleistocene. This aquifer is 20–40 m thick and overlays a clayey-silty aquitard, which has a highly variable thickness, and partially confines the underlying aquifer in the southern sector of the plain. The underlying semi-confined aquifer (Aquifer Group B) is 40–60 m thick and consists of sands and sandy gravels of high-energy fluvial environments, with origins generally from north to south, dated as Middle Pleistocene. The semi-confined aquifer overlays clay and silt layers and locally conglomeratic units. This layers of fine sediments have a thickness ranging between 5 and 50 m, increasing from north to south and represents an aquitard or aquiclude between Aquifer Groups B and C. The deep confined aquifer (Aquifer Group C) consists of sandy lenses within clay and silt units representing the Early Pleistocene from marine to continental transition facies.

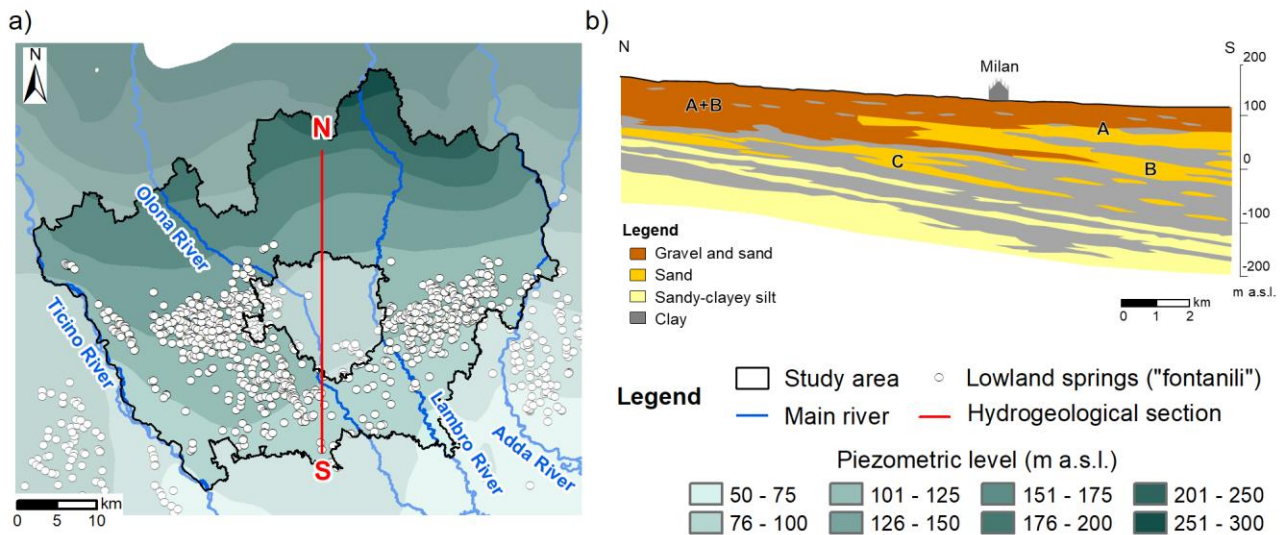


Fig. 2 – a) Piezometric levels of the shallow aquifer (m a.s.l.) and location of the lowland springs (“fontanili”); b) North-south hydrogeological section. In the northern sector of the study area, Aquifer Groups A and B constitute a unique unconfined aquifer (A+B). Proceeding toward south, the unconfined shallow Aquifer Group A is gradually separated from the underlying semi-confined Aquifer Group B by an aquitard. Aquifer Group C represents the confined deep aquifer.

The groundwater flow is generally oriented north-south (Fig. 2a) and is influenced by the main rivers, acting prevalently as gaining streams (Alberti et al., 2016b). The groundwater table depth decreases from north to south, ranging between values higher than 70 m to less than 2 m below ground level (b.g.l.). Moving between the higher and the lower plain, a 20 km-wide belt is characterised by the presence of lowland springs (“fontanili”) due to the decrease in both grain size, transitioning from coarse sandy gravel to medium-fine sand, and in transmissivity (Fig. 2b, De Luca et al., 2014).

Domestic, commercial, industrial and agricultural activities of this densely populated area show a clear impact both on availability and quality of groundwater resources (Sacchi et al., 2013; Alberti et al., 2016a; De Caro et al., 2017). In particular, the study area is one of the most urbanised and industrialised areas in Europe affected by chlorinated-hydrocarbon contamination (i.e., PCE, TCE) and Cr(VI) contamination (Provincia di Milano, 2002; Beretta and Bianchi, 2004; Pedretti et al., 2013; Gorla et al., 2016; Azzellino et al., 2019). Gruppo CAP, a public company owned by local authorities, manages the integrated water service in around 200 municipalities of the Milan Metropolitan area, with a customer base of about 2.5 million inhabitants. As part of the managing activities of the groundwater resource,

Gruppo CAP monitors the hydrochemical characteristics of groundwater on a monthly basis. The hydrochemical dataset covers the period 2003–2016 and includes 96,827 records with 107 attributes of chemical analyses from drinking water well samplings. The database includes water well coordinates, sampling date, and a code indicating the Aquifer Group to which each record belongs.

Data collected in 2016 are used in this study. The average concentrations of PCE+TCE and Cr(VI) are calculated for each well screened in the shallow or deep aquifers. Figure 3a and b show the distribution of PCE+TCE and Cr(VI) in the shallow aquifer. Figure 3c and d show the distribution of the contaminants in the deep aquifer. This indicates a situation of groundwater diffuse contamination where contaminants are present over large sectors of the study area.

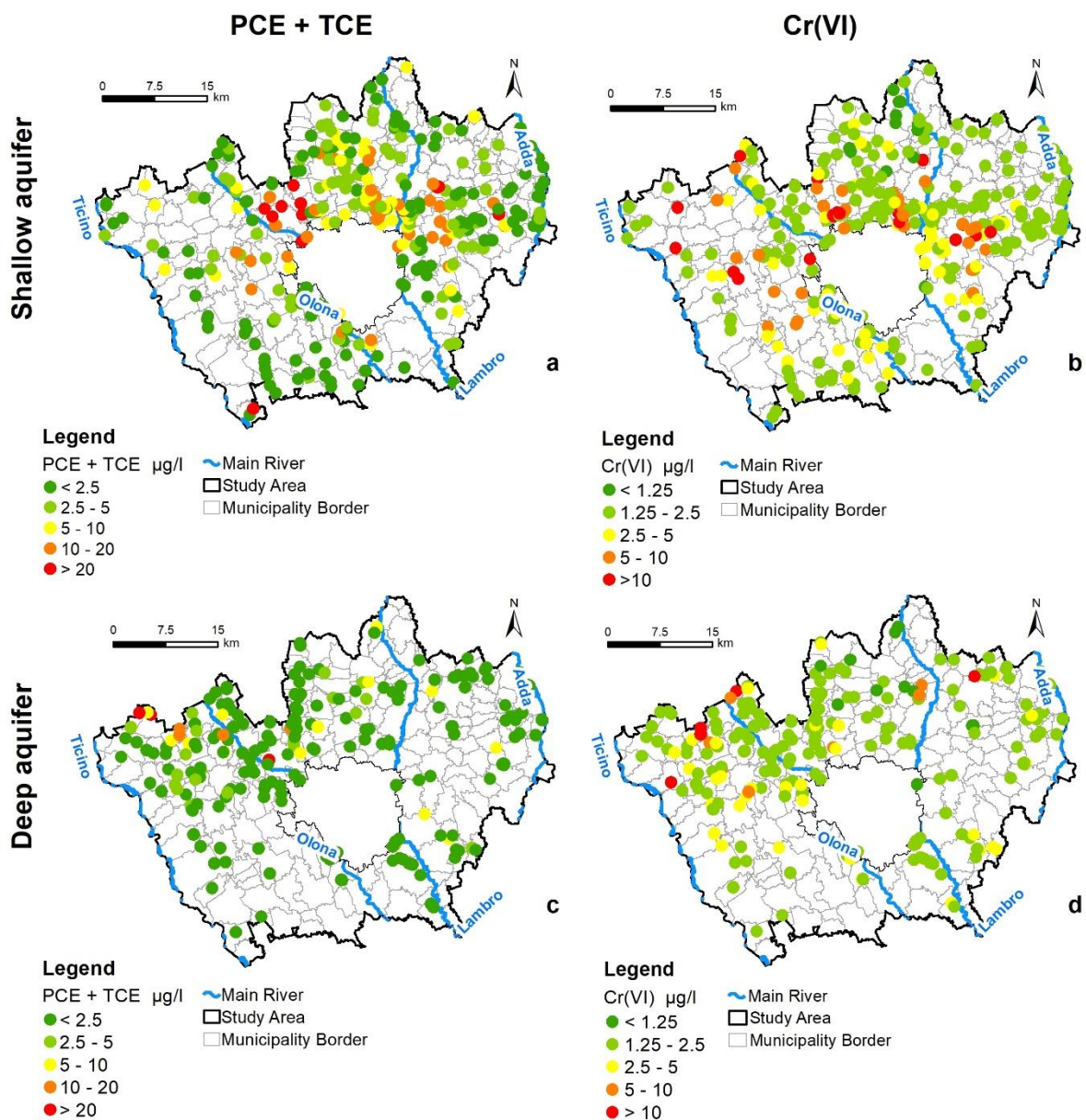


Fig. 3 – a) Groundwater average concentration of PCE+TCE in the 2016 shallow aquifer (Groups A and B); b) Groundwater average concentration of Cr(VI) in the 2016 shallow aquifer (Groups A and B); c) Groundwater average concentration of PCE+TCE in the 2016 deep aquifer (Group C); d) Groundwater average concentration of Cr(VI) in the 2016 deep aquifer (Group C).

### **3 Methods and materials**

#### **3.1 Weights of Evidence theory and analysis procedure**

The Weights of Evidence (WofE) technique is defined as a data-driven Bayesian method in a log-linear form that can be used to generate predictive models based on the combination of multiple spatial data and on the concepts of prior and posterior probability (Bonham-Carter, 1994; Raines, 1999).

In this study, the WofE technique has been applied to assess and map both shallow and deep aquifer susceptibility to PCE+TCE and Cr(VI) contamination. The power of this technique is that it can be used to quantify the role and the importance of specific factors (evidential themes) in conditioning the occurrence of high pollutant concentrations (training points) in groundwater.

The WofE method has been executed using the Arc Spatial Data Modeler (ArcSDM; Sawatzky et al., 2009) extension within the ESRI ArcGIS 10.0 software (ESRI, 2010) following the procedure described below:

- 1) *Creation of a large database.* In order to apply the WofE technique, it is necessary to collect a large number of spatial data concerning factors (e.g., contaminant load, groundwater table depth) potentially affecting groundwater quality and the distribution of PCE+TCE and Cr(VI) concentrations in shallow and deep aquifers;
- 2) *Statistical analysis on concentration data of each contaminant.* This analysis is done to identify:
  - i) training points (TPs) used to both generate and calibrate the final model, and ii) control points (CPs), adopted only during the validation procedure;
- 3) *Calculation of the prior probability.* The study area is subdivided in unit areas (i.e., cells) of the same extensions. The prior probability represents the probability that a cell contains a TP without considering any existing evidential theme (Bonham-Carter, 1994);

- 4) *Generalisation of evidential themes.* Each evidential theme is generalised into classes, each one representing a different range of values. For each single class, positive  $W^+$  and negative  $W^-$  weights, and contrast and confidence values are calculated. The difference between  $W^+$  and  $W^-$  defines the contrast, an overall measure of the degree of the spatial correlation among TPs and each class of the evidential theme: a positive contrast identifies a direct correlation between the class and the TPs, a negative contrast defines an inverse correlation, whereas a contrast value close to zero means low or no correlation. The confidence is given by the ratio between the contrast and its standard deviation and provides a useful measure of the significance of the contrast and, thus, of the respective class (Raines, 1999). In order for a class to be considered statistically significant, it must be characterised by a confidence value higher than the test value, which is established at the beginning of the analysis and reflects a specific level of significance. In this study, a test value of 1.645, almost corresponding to a 95% level of significance, was adopted to assess the susceptibility of both shallow and deep aquifers to PCE+TCE and Cr(VI) contaminations. Each evidential theme is repeatedly reclassified in order to obtain the maximum number of statistically significant classes. The reclassification procedure was carried out by adopting the same technique proposed and described by Sorichetta et al. (2012);
- 5) *Evaluation of the physical significance of the evidential themes.* To perform the susceptibility analysis with the WofE technique, it is necessary that the evidential themes, selected as input, show a statistically as well as a physically significant correlation with the occurrence of high pollutant concentrations. This means that the relationship found between the contamination and a specific class of the considered evidential theme must prove to be consistent with the hydrogeological processes that influence groundwater pollution;
- 6) *Generation of the predictive probability models and their conversion to susceptibility maps.* At the end of the analysis, four predictive models are generated, resulting from the combination of statistically and physically significant evidential themes. Each output shows the distribution of the posterior probability values corresponding to the relative probability that a cell within the study area contains a TP based on the evidence provided by the evidential themes. The posterior probability can be expressed as:

$$\log_e O\{D|B_1^k \cap B_2^k \cap B_3^k \dots \cap B_n^k\} = \sum_{j=1}^n W_j^k + \log_e O\{D\}$$

where  $n$  indicates each single class used to categorise each evidential theme,  $k$  is either + or – depending on whether the prediction spatial class,  $B_n$ , is either present or absent, and  $O\{D\}$  is the odd form of the probability that a cell within the study area contains an occurrence.

The concept of relative probability indicates that areas of higher posterior probability are more likely to contain a TP than areas of lower posterior probability (Bonham-Carter, 1994; Raines, 1999). Each predictive model is reclassified using the geometrical interval method, which ensures that each class contains approximately the same number of different posterior probability values (Sorichetta et al., 2011). The reclassified susceptibility map consists of five classes, with the degree of susceptibility increasing from 1 to 5. This number is selected based on the general criteria used to identify vulnerability classes (Sorichetta et al., 2011) and on visual analytic techniques (Cowan, 2001). The reclassified susceptibility map can be used to identify areas with a high degree of susceptibility and, thus, with a high posterior probability value, where contamination is more likely to occur as a function of the presence of specific classes of each evidential theme;

- 7) *Calibration and validation of the posterior probability and susceptibility maps.* The accuracy and reliability of the final maps are analysed using the following procedures: i) the area-under-the-curve (AUC) technique (Chung and Fabbri, 1999), ii) the frequency of training set, and iii) the average concentration of PCE+TCE and Cr(VI) in all the wells located within each susceptibility class.

The AUC technique describes the accuracy of the posterior probability map in correctly classifying the occurrence of the TPs. The AUC value is given by the area under the curve within the diagram generated by plotting, on the X-axis, the cumulative percentage of susceptible areas and, on the Y-axis, the cumulative percentage of training points. According to Pourghasemi et al. (2013), the relationship between AUC value and degree of accuracy can be classified as follows: 0.9–1, excellent; 0.8–0.9, very good; 0.7–0.8, good; 0.6–0.7, average; and 0.5–0.6, poor.

The performance of each reclassified susceptibility map is examined by considering its global performance in classifying the occurrences through: i) the frequency of TPs and ii) the average concentration of the pollutants in each susceptibility class (Sorichetta et al., 2011). These two methodologies are based on the use of all the wells, both TPs and CPs. The frequency of TPs is expressed as the ratio between the number of TPs in a susceptibility class and the total number of wells in the same susceptibility class. The average concentration is derived from the ratio between the sum of concentration values measured in wells located in a susceptibility class and the total number of concentration data collected within the same susceptibility class. Both the frequency of TPs and the average concentration are expected to monotonically increase as the degree of susceptibility increases (from class 1 to 5). The reliability of each map is verified by considering both the angular coefficient of the regression line and its regression coefficient within each histogram.

### **3.2 Conceptual model**

Due to the total absence of the aquitard between Aquifer Groups A and B in the northern part of the study area and to the considerable variability of its thickness, in this study, Aquifer Groups A and B were considered as a unique aquifer, representing the shallow aquifer. Whereas, the underlying Aquifer Group C identifies the deep aquifer. Shallow and deep aquifers were analysed independently according to the adopted conceptual model. To assess groundwater susceptibility, the WofE technique required the use of a factor to be considered as a potential source of contamination. Potential sources of PCE+TCE and Cr(VI) in groundwater include industrial and commercial activities such as automotive, refineries, chemical and steel plants, tire production, and wet and dry cleaning activities.

Observing the scenario shown in Figure 4, we considered industrial spillage as the main cause of contaminant release into the shallow aquifer (i.e., direct source), together with commercial and artisanal settlements related to chlorinated solvents and Cr(VI) use.

Considering the deep aquifer, we hypothesised that waters enriched in PCE+TCE and Cr(VI) within the shallow aquifer can aggravate the qualitative status of the deep aquifer. This means that the upper

aquifer can represent a secondary (i.e., indirect) source responsible for the contamination of the underlying deep aquifer. Together with polluted waters in the shallow aquifer, local heterogeneities in the aquitard and wells exploiting both aquifers (i.e., multi-aquifer wells) can have a relevant role in favouring the vertical migration of the contaminants, thus compromising the quality of the deep aquifer (Johnson et al., 2011; Filippini, 2017). Heterogeneities of the aquitard can include sectors with reduced thickness of fine sediments or zones where the layer is mainly comprised of a silty-sandy matrix (i.e., more permeable than a clay matrix), so that, locally, the vertical groundwater flow through the aquitard is favoured with respect to the horizontal groundwater flow. Multi-aquifer wells are designed to exploit aquifers separated by impermeable layers to minimise the perturbation of the natural hydrogeological system. However, this perturbation can cause preferential vertical flows along the borehole walls, inducing a connection between the upper and lower aquifers.

To complete the framework of the conceptual model, we assumed that Cr(VI) prevalently remains in its oxidized form. The historical presence and persistence of this Cr form in the study area (Giovanardi, 1979; Provincia di Milano, 1992) indicates that aquifers conditions tend to favour the maintenance of this Cr form. However, it cannot be excluded that local conditions with ferrous iron minerals, reduced sulphur, and soil organic matter can create less oxidized phase (Palmer and Puls, 1994), in some specific small areas. The same historical evidence is valid for PCE+TCE, that are the most relevant and persistent chlorinated solvents in the study area (Giovanardi, 1979; Provincia di Milano, 1992). Also, in this case the natural attenuation of these compounds cannot be completely excluded. Anyway, the use of the sum PCE+TCE (instead of the concentration of the single compound) allows to indirectly take into account part of the degradation chain (from PCE to TCE) that does not affect the value of the sum of the two compounds.

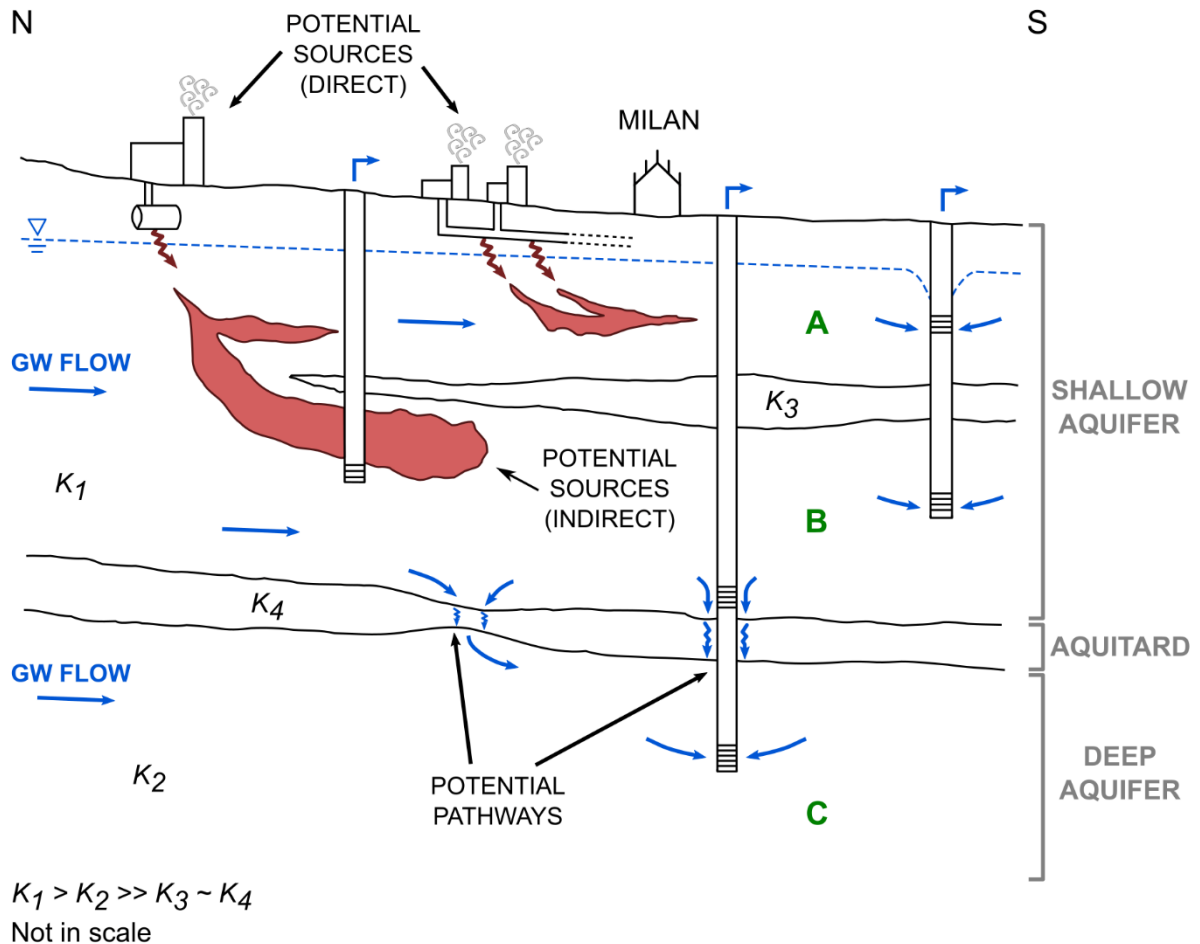


Fig. 4 – Conceptual hydrogeological model.

### 3.3 Training points and control points

In this study, the mean pollutant concentration detected during the year 2016 was assigned to each well. As a first step, a statistical analysis was performed examining the frequency distribution of both PCE+TCE and Cr(VI) concentrations in each single aquifer (Table 1). The aim of this analysis was to define the median value, generally selected as the concentration threshold value in the WofE method (Masetti et al., 2009). This value allowed to distinguish two populations, as required by the WofE technique: wells considered as TPs, for the implementation of the models, and wells identified as CPs, for the calibration and validation phase.

Considering the PCE+TCE concentration data, the median value of 1.0  $\mu\text{g/l}$  was used as threshold in the deep aquifer to identify 107 wells, with concentrations higher than or equal to 1.0  $\mu\text{g/l}$ , as TPs, and 148 wells, with concentrations lower than 1.0  $\mu\text{g/l}$ , as CPs. Although a median value of 3.2  $\mu\text{g/l}$  was

obtained in the shallow aquifer, the concentration value of 4.0 µg/l was identified as the most appropriate value to use as a threshold. In this case, the use of cumulative probability plots (Sinclair, 1974; Panno et al., 2006; Masetti et al., 2009) allowed to distinguish two different populations within the dataset by considering the inflection point (i.e., 4.0 µg/l) of the cumulative curve as threshold value. Thus, 154 wells, with concentrations higher than or equal to the threshold value, were used as TPs, while 224 wells, with concentrations lower than the threshold value, were considered as CPs.

Taking into account the occurrence of Cr(VI) in groundwater, the median concentration value (2.5 µg/l) was adopted as the threshold for the analyses performed both on the shallow and the deep aquifer. In this case, due to the high presence of wells characterised by a Cr(VI) concentration of 2.5 µg/l (218 out of a total of 380 wells in the shallow aquifer and 174 out of a total of 253 wells in the deep aquifer), it was found more appropriate to consider only wells above the threshold value as TPs. In this way, it was possible to define a significant number of both TPs and CPs, in order to perform the WofE analysis. Therefore, in the shallow aquifer, 126 wells resulted as TPs and the remaining 254 were used as CPs, whereas, in the deep aquifer, 54 wells were identified as TPs and the remaining 199 were considered as CPs.

<b>Contaminant</b>	<b>Shallow aquifer</b>	<b>Deep aquifer</b>	<b>Statistics</b>	<b>Drinking water limit (D. Lgs. 152/06)</b>	<b>Drinking water limit (Drinking Water Directive - 98/83/EC)</b>
<b>PCE+TCE (µg/L)</b>	1.0	1.0	Min	10 µg/l	10 µg/l
	77.5	59.4	Max		
	5.5	3.3	Mean		
	3.2	1.0	Median		
	4.8	5.4	Skewness		
	7.5	7.4	Std. Dev.		
<b>Cr(VI) (µg/L)</b>	0.5	0.5	Min	5 µg/l	50 µg/l (Total Chromium)
	45.0	27.2	Max		
	3.9	3.1	Mean		
	2.5	2.5	Median		
	4.8	5.7	Skewness		

	4.3	2.7	Std. Dev.		
--	-----	-----	-----------	--	--

Table 1 – Statistics of PCE+TCE and Cr(VI) contamination, expressed in µg/L, measured in the shallow and deep aquifers and referred to the 2016 monitoring campaigns.

### 3.4 Evidential themes

Based on the conceptual hydrogeological model, seven evidential themes are considered as factors influencing groundwater susceptibility to PCE+TCE and Cr(VI) contamination in the study area in both the shallow and deep aquifers. These variables, representing both natural and anthropogenic factors (Table 2, Supplementary Material 1), were derived from multiple sources of information. These variables were selected to capture the pathway and the main regional-scale processes that characterise the contamination pattern (Stevenazzi et al., 2017). For the shallow aquifer, this includes potential release from the surface (primary source) and eventual protection of the aquifer, represented by local discontinuous aquitard levels within the aquifer (degree of confinement), vertical spreading (hydraulic conductivity of the vadose zone) to the saturated zone (groundwater table depth), and transport and dilution in the aquifer (groundwater flow velocity). For the deep aquifer, this includes pollutant distribution in the shallow aquifer (secondary source), potential leakages from the shallow to the deep aquifer through multi-aquifer wells (areal density of multi-aquifer wells), and level of protection of the deep aquifer, represented by the thickness of the aquitard between the shallow and the deep aquifer. The importance of each variable in influencing groundwater susceptibility can change for each contaminant depending on the location of the real sources related to it and to the abilities of the specific contaminant to be transported as a solute in groundwater (considering the concentrations that are not so high to allow the formation of DNAPL for chlorinated solvents). Moreover, the importance of each variable can differ according to its local spatial relation with the other variables.

The **groundwater table depth** map of the shallow aquifer was created by calculating the difference between the topographic surface and the groundwater piezometric level; the latter generated by kriging interpolation with trend analysis of the piezometric measurements (Goovaerts, 1997). In the study area, the groundwater table depth ranges from 0 to 70 m b.g.l.. High values occur in the north sector and gradually decrease moving to the south sector. As shown in literature (e.g., Arthur et al., 2007; Mendoza

and Barmen, 2006; Shrestha et al., 2016), a near-surface groundwater table decreases the vertical distance through which the contaminant must travel before reaching groundwater.

The **hydraulic conductivity of the vadose zone** map was obtained by interpolating some experimental data from borehole tests together with values derived from well stratigraphy records through the equivalent vertical permeability method (Anderson and Woessner, 1992), considering the thickness of the layers in the vadose zone. Within the study area, the hydraulic conductivity of the vadose zone ranges from  $3.2 \times 10^{-10}$  to 0.12 m/s and represents the equivalent vertical saturated hydraulic conductivity through the vadose zone. Generally, areas characterised by a high hydraulic conductivity of the vadose zone contribute to facilitate the vertical migration of the contaminant towards the saturated zone.

The **groundwater flow velocity** map was determined using the hydraulic conductivity data obtained from pumping tests together with the local hydraulic gradient. In the study area, the groundwater flow velocity ranges from  $8.9 \times 10^{-9}$  to  $2.1 \times 10^{-5}$  m/s. Previous studies (e.g., Uhan et al., 2011; Sorichetta et al., 2012; Stevenazzi et al., 2015) showed that zones with high groundwater flow velocity are more likely to be associated with contaminated areas. This suggests that the transport of the contaminant over large areas prevails over dilution process.

The map representing the **degree of confinement** was generated by dividing the study area into three classes of “low”, “medium” and “high” degree. Each class reflects the presence of a fine sediment layer that determines the gradual transition from the unconfined shallow aquifer (Groups A and B) to the semi-confined shallow aquifer (Group B). In the study area, the degree of confinement increases from north to south, in agreement with the characteristics of the hydrogeological structure of the subsoil. The presence of low permeability levels can serve as an effective barrier to prevent the vertical transport of contaminated waters coming from the surface in the lower part of the shallow aquifer. At the same time, it reduces the transmissivity of the upper part of the shallow aquifer making the process of contaminant dilution less efficient.

The map showing the **extent of potential sources zones (PSZ) of chlorinated compounds and Cr(VI)** in 2015, expressed as percentage, was derived considering the class “industrial, artisanal and commercial settlements” within the regional land use inventory (ERSAF, 2018) and using the same

procedure described in Pollicino et al., 2019. We use this variable for PCE+TCE and Cr(VI) because it includes in one single group all the potential sources related to both contaminants, even if the single source could be related to only one of the two contaminants. No more detailed data are available to separate the potential sources of PCE+TCE from the ones related to Cr(VI) only.

The map of the **thickness of the aquitard** that separates the shallow aquifer from the deep aquifer was obtained through the spatial interpolation of data representing the thickness of the aquitard derived from 500 well logs. This aquitard separates Aquifer Group B from the underlying Aquifer Group C. In the study area, the aquitard thickness ranges from 0 to 50 m. In areas where the thickness of the aquitard is reduced, the deep aquifer is less protected and, thus, more exposed to the propagation of the contaminant coming from the overlying aquifer.

**Contaminant concentrations in the shallow aquifer** (Aquifer Group A+B) measured during the 2016-monitoring campaign were used to generate the maps of contaminant distribution of PCE+TCE and Cr(VI). The maps were obtained through the interpolation of concentration data using the inverse distance weighted method.

The map representing **potential leakages from the shallow aquifer system** (Aquifer Group A+B) to the deep one (Aquifer Group C) was generated considering that the high presence of wells screened in both aquifers can contribute to the deterioration of the water quality in the deep aquifer, favouring the movement of the pollutant towards the deeper strata. As a first step, wells screened in both aquifers (multi-aquifer wells) were selected in the database. A semicircular buffer of 5 km<sup>2</sup> was created around (i.e., upgradient) each multi-aquifer well. The total number of multi-aquifer wells located within the buffer was defined and then assigned to the multi-aquifer well at the centre of the semicircle. Then, a categorical map consisting of 11 classes was obtained by interpolating the values through the inverse distance weighted method. In this map, each class reflects the areal density of multi-aquifer wells expressed as the total number of wells exploiting both shallow and deep aquifers per 5 km<sup>2</sup>.

	<b>Evidential theme</b>	<b>Type</b>	<b>Minimum</b>	<b>Maximum</b>
<b>Shallow Aquifer</b>	Groundwater table depth (m b.g.l.)	Numerical	0	70
	hydraulic conductivity of the vadose zone (m/s)	Numerical	$3.2 \times 10^{-10}$	0.12
	Groundwater flow velocity (m/s)	Numerical	$8.9 \times 10^{-9}$	$2.1 \times 10^{-5}$
	Degree of confinement	Categorical	-	-
	Potential sources zone (%)	Numerical	0	100
<b>Deep Aquifer</b>	Thickness of the aquitard between shallow and deep aquifers (m)	Numerical	0	50
	PCE+TCE concentration in the shallow aquifer ( $\mu\text{g/l}$ )	Numerical	1	74
	Cr(VI) concentration in the shallow aquifer ( $\mu\text{g/l}$ )	Numerical	1	43
	Number of multi-aquifer wells per 5 km <sup>2</sup>	Numerical	0	11

Table 2 – Evidential themes used in the WofE analysis on shallow and deep aquifer susceptibility to PCE+TCE and Cr(VI) contamination.

## 4 Results

### 4.1 Contrasts of the generalised evidential themes

Although the analysis on contrasts has been performed adopting a 95% level of significance, some of the investigated evidential themes have shown to have no significance from a statistical point of view. In order to consider the contribution of these statistically insignificant evidential themes, it was necessary, in these cases, to decrease the level of significance to 90%. In the assessment of shallow aquifer susceptibility, all the evidential themes were found to be statistically significant at a 95% level of significance, except for the factors representing the hydraulic conductivity of the vadose zone (in the case of PCE+TCE contamination) and the groundwater flow velocity (in the case of Cr(VI) contamination). In the assessment of deep aquifer susceptibility, all the evidential themes proved to be statistically significant at a 95% level of significance, except for the factor concerning the thickness of the aquitard in the case of PCE+TCE contamination.

The individual role of each evidential theme in influencing groundwater contamination was evaluated by considering, for each evidential theme, the contrast of each statistically significant class. Considering the evidential themes that control the susceptibility of the shallow aquifer to PCE+TCE and Cr(VI) contamination, histograms show a direct correlation between high concentrations of both contaminants and (Fig. 5):

- high values of groundwater flow velocity;
- high values of hydraulic conductivity of the vadose zone;
- low values of groundwater table depth (roughly less than 30 m b.g.l.);
- a medium or medium-high degree of confinement;
- high presence of “potential sources zone” (>5%).

The results derived from the analysis on evidential themes that can influence the susceptibility of the deep aquifer indicate a direct relationship between high concentrations of both pollutants and (Fig. 6):

- low thickness of the aquitard separating shallow and deep aquifers (roughly less than 30 m);
- areas where the shallow aquifer contains high PCE+TCE (>17 µg/l) and Cr(VI) (>5 µg/l) concentrations;
- presence of wells screened in both shallow and deep aquifers (equal or more than two multi-aquifer wells in 5 km<sup>2</sup>).

## Shallow aquifer

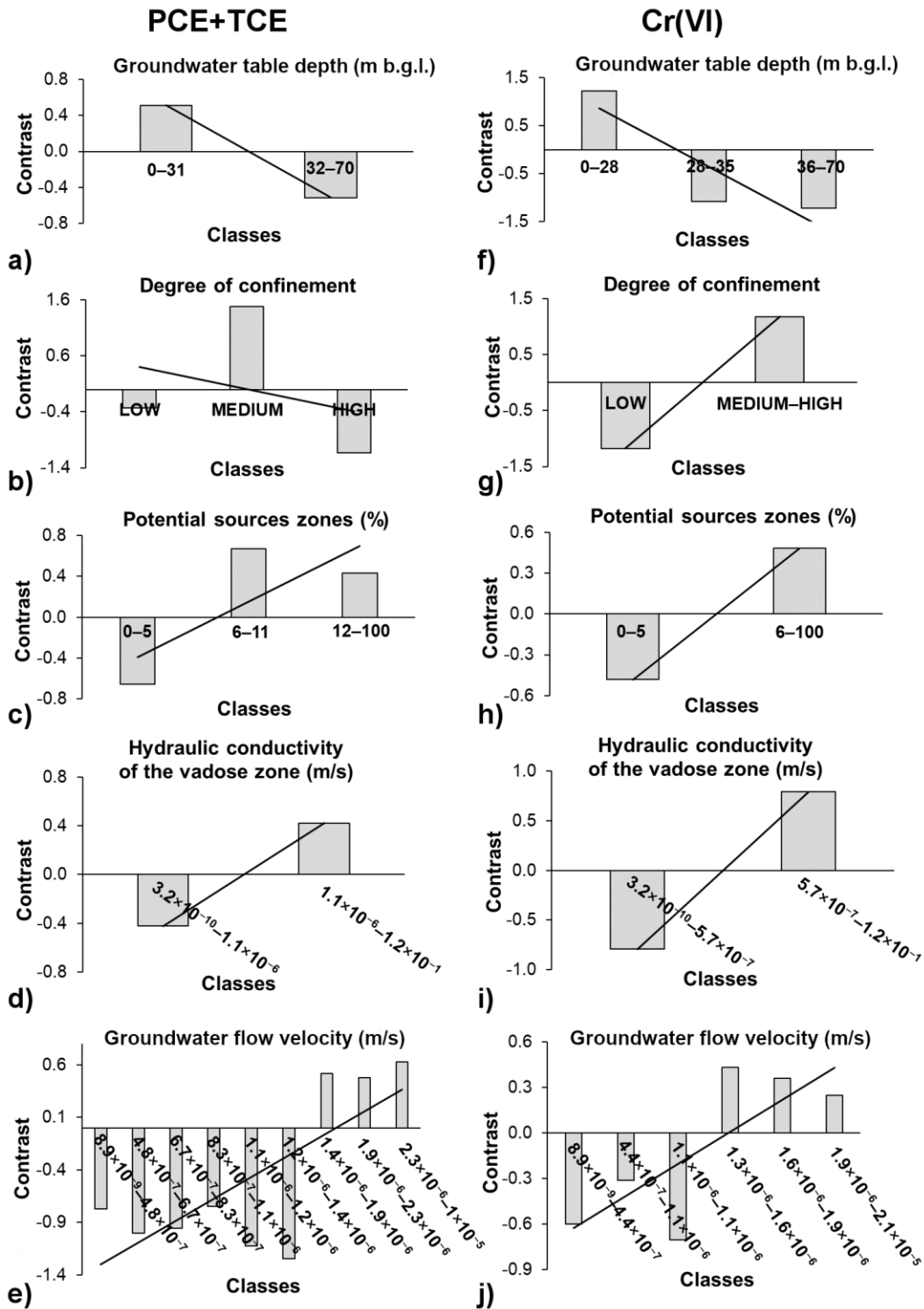


Fig. 5 – Contrasts of each statistically significant class of each evidential theme. Histograms represent the contrasts of the evidential themes that influence shallow aquifer susceptibility to PCE+TCE (a–e) and Cr(VI) (f–j) contamination.

## Deep aquifer

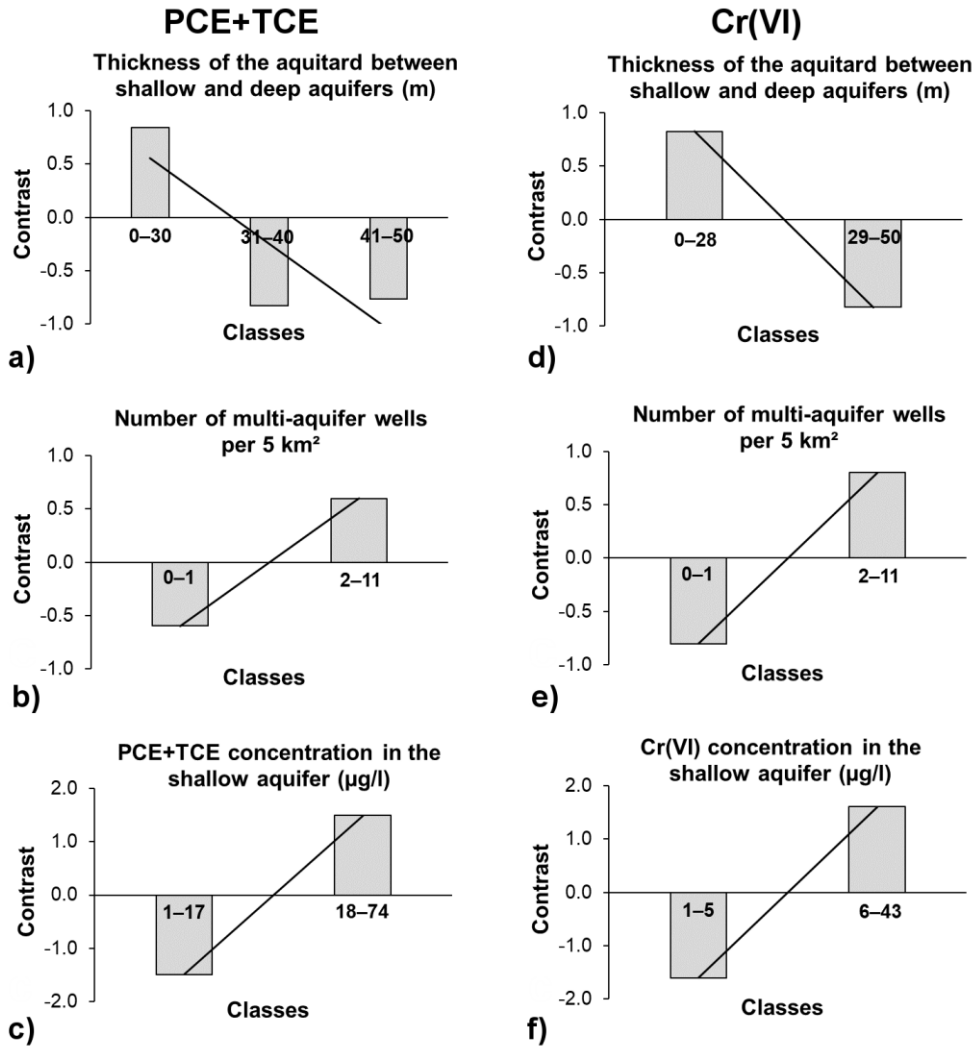


Fig. 6 – Contrasts of each statistically significant class of each evidential theme. Histograms represent the contrasts of the evidential themes that control deep aquifer susceptibility to PCE+TCE (a–c) and Cr(VI) (d–f) contamination.

### 4.2 Susceptibility maps and their reliability

In order for an evidential theme to be used as input to generate the predictive models it is necessary that it shows both statistical and physical significance. In this study, all the investigated evidential themes were found to be statistically significant and their relationship with the pollution proved to be defensible and justifiable from a physical (i.e., hydrogeological) point of view. Only the degree of confinement variable provided a counterintuitive result that will be analysed in the discussion section.

Despite this, all the evidential themes were considered and combined to generate the posterior probability maps subsequently converted into susceptibility maps (Fig. 7).

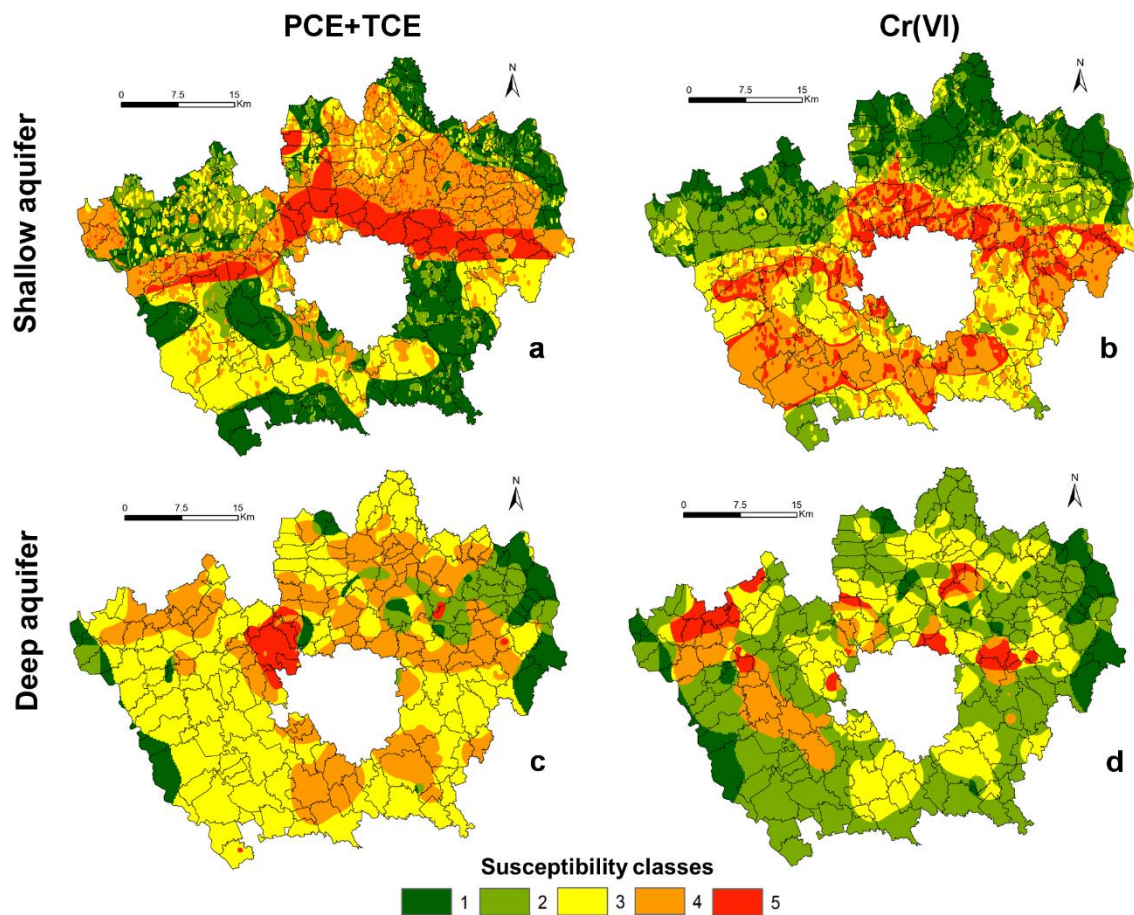


Fig. 7 – Reclassified susceptibility maps. Maps (a) and (b) represent the shallow aquifer susceptibility to PCE+TCE and Cr(VI) contamination, respectively. Maps (c) and (d) represent the deep aquifer susceptibility to PCE+TCE and Cr(VI) contamination, respectively. In each map the degree of susceptibility increases from class 1 (green) to 5 (red).

Before analysing the reliability of the reclassified susceptibility maps, the accuracy of each posterior probability map was evaluated by using the AUC technique. The AUC analysis performed on PCE+TCE posterior probability maps provided AUC values equal to 74.5% for the shallow aquifer case and 64.8% for the deep aquifer case. Whereas, the AUC technique applied on Cr(VI) posterior probability maps showed AUC values equal to 69.0% for the shallow aquifer case and 71.6 % for the deep aquifer case.

All the histograms of the average concentration method show that, despite some anomalies, the average PCE+TCE and Cr(VI) concentration increases according to the degree of susceptibility, as expected. Histogram (a) in Figure 8 reveals an anomaly related to class 3, which shows an average PCE+TCE concentration value lower than that of class 2. A further anomaly has been found within histogram (b) in Figure 8 and is represented by class 4, characterised by an average Cr(VI) concentration value higher than that of class 5. All the histograms derived from the average concentration provided regression coefficient values higher than or equal to 0.85, except for the histogram derived from the validation of the deep aquifer susceptibility map to PCE+TCE pollution (Fig. 8a), which shows a regression coefficient equal to 0.66.

Focusing on the frequency of TPs in each susceptibility class, all the histograms highlight that, although some anomalies have been identified, the frequency of TPs increases from susceptibility class 1 to 5. Histogram (c) in Figure 8 shows an anomaly related to class 3, characterised by a frequency of TPs higher than that of class 4, whereas histogram (d) in Figure 8 reveals an anomaly represented by class 4, characterised by a frequency of TPs higher than that of class 5. Examining the regression coefficient within each histogram, they have provided values higher than or equal to 0.82, except for the histogram obtained from the validation of the shallow aquifer susceptibility map to Cr(VI) contamination (Fig. 8d), which shows a regression coefficient equal to 0.67.

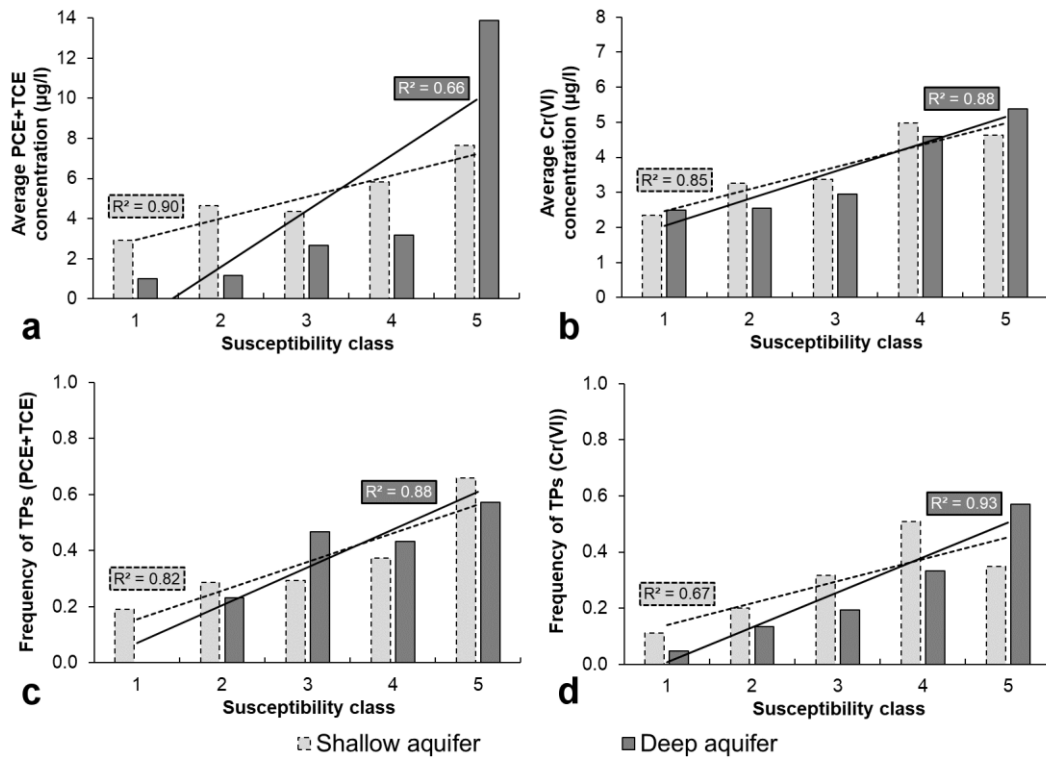


Fig. 8 – Validation procedures applied on the reclassified susceptibility maps: (a–b) average concentration method; (c–d) frequency of training points (TPs) method.

## 5 Discussion

In environmental and decision-making contexts, the delineation of both potential source zones and highly susceptible areas at a regional scale can provide an essential contribution to achieve a sustainable management of urban groundwater. This information becomes even more important when it reveals a decrease in the protection (i.e., an increase in the susceptibility) of the deep aquifer, normally recognised as a long-term safe source of drinking water. The development of shallow and deep aquifers susceptibility maps at regional scale can offer an efficient support for the identification of areas where a more detailed investigation is required. The good performance of the maps in correctly representing the distribution of the degree of susceptibility within the study area has been highlighted by the satisfactory results derived from the AUC and the validations techniques, especially for maps representing the shallow aquifer susceptibility to PCE+TCE contamination (Fig. 7a) and the deep aquifer susceptibility to Cr(VI) contamination (Fig. 7d).

The analysis on contrast values performed with the WofE method revealed the existence of the same relationship between the investigated evidential themes and the occurrence of high concentrations levels of both PCE+TCE and Cr(VI) in both the shallow and deep aquifer. Except for the degree of confinement variable, the correlation found between each individual evidential theme and PCE+TCE and Cr(VI) contamination proved to be in line with the expected results and were compared with the outcomes obtained in other groundwater vulnerability studies to non-point sources of contamination (e.g., Arthur et al., 2007) or multiple-point sources of contamination (e.g., Mair and El-Kadi, 2013; Rajput et al., 2020). For PCE+TCE contamination, this outcome is also related to the fact that areas with diffuse PCE+TCE contamination are characterized by concentrations higher than the drinking water limit but far from forming a separate phase. Thus, this means that, under this condition, PCE+TCE moving in groundwater behaves as a solute.

For the shallow aquifer, we observed that areas with high groundwater flow velocity, high hydraulic conductivity of the vadose zone and low groundwater table depth contribute to enhance the migration and transport of PCE+TCE and Cr(VI) in groundwater. More specifically, contrast values revealed that areas with groundwater table depth lower than 28–31 m and groundwater flow velocity higher than  $1.3 \times 10^{-6}$ – $1.4 \times 10^{-6}$  m/s could create ideal conditions for the occurrence of high concentrations of both contaminants. Although the study carried out by Rajput et al. (2020) highlighted a weak influence of both groundwater table depth and vadose zone on the distribution of chromium concentrations, in this study, these variables proved to have a significant impact on Cr(VI) mobilisation within the area of interest. Considering PCE+TCE contamination, groundwater flow velocity provided contrast values higher than the other evidential themes, suggesting a stronger influence of this variable in controlling the transport of the contaminant into the aquifer. The positive relationship found between the contamination due to chlorinated compounds and groundwater flow velocity had already been observed in Pollicino et al. (2019), in which aquifer susceptibility to diffuse PCE contamination had been assessed at a municipal scale.

As showed in other works (e.g., Moran et al., 2007; Rivett et al., 2012; Mair and El-Kadi, 2013), the direct relationship obtained between chlorinated solvents and Cr(VI) contamination and the high presence of PSZ (i.e., direct sources) has confirmed the severe pressure that human activities impose

on groundwater resources. Contrast values indicated that areas characterised by an areal density of industrial and commercial activities higher than 6% may negatively affect the quality of groundwater bodies. The assessment of the role of specific variables on the susceptibility of the deep aquifer has reinforced the importance of recognising the shallow aquifer as a secondary (i.e., indirect) source responsible for the contamination of the underlying deep aquifer by decreasing its degree of protection. In both deep aquifer susceptibility maps (Fig. 7c,d), the distribution of the degree of susceptibility within the study area seems to be important in controlling the occurrence of PCE+TCE and Cr(VI) in the shallow aquifer.

The infiltration of polluted water from the upper to the underlying aquifer can be enhanced by both the presence of thickness reduction in the aquitard separating the two aquifers and inappropriate design of multi-aquifer wells. The histograms in Figure 6 showed that areas with a thickness of the aquitard lower than 30 m and more than 2 multi-aquifer wells per 5 km<sup>2</sup> may create preferential conditions for contaminant transport in the deep aquifer. Although it is critical to be evaluated on a large scale, we cannot exclude the potential effect due to the historical accumulation of DNAPL source zones on aquitard top and their subsequent migration through preferential flowpaths within the aquitard (White et al., 2008).

The degree of confinement seems to be significant in identifying susceptible and not susceptible areas in the shallow aquifer susceptibility maps (Fig. 7a,b). In contrast with what we expected, the most critical areas correspond to those with a medium (for PCE+TCE) or medium-high (for CrVI) degree of confinement. On the one hand the results could be influenced by the different action that this variable can have on the two different part of the shallow aquifer in terms of susceptibility, as reported in Section 3.4. On the other hand, the result could be related to the long history of industrial and commercial activities, which were relevant from the 1960s in the area corresponding to the one with a medium degree of confinement. Although these activities were dismantled decades ago, they have been acted as potential sources of contamination for years, but the lack of information on these activities does not allow to use them in this analysis. In the map representing the shallow aquifer susceptibility to Cr(VI) contamination (Fig. 7b), the most critical areas also affect the entire southern sector of the study area.

This could be a result of the combined effect associated with the presence of historical sources located upstream and the high mobility of the contaminants in groundwater flow generally oriented north-south.

## **6 Conclusions**

On the basis of this study, it is possible to conclude that:

- the WofE method has proved to be effective and reliable to assess the quality deterioration of both shallow and deep aquifers due to diffuse contamination at a regional scale;
- the susceptibility of the shallow aquifer to the presence of diffuse contamination is controlled by the combination of high groundwater flow velocity, high hydraulic conductivity of the vadose zone and low groundwater table depth;
- the shallow aquifer can be considered as a secondary source responsible for the deterioration of deep aquifer quality;
- the WofE method allowed to quantify the impact exerted by the morphological heterogeneities in the aquitard between shallow and deep aquifers and the inappropriate design of multi-aquifer wells in facilitating the mobilisation of contaminated waters from the upper to the underlying aquifer through preferential flowpaths;
- historical anthropogenic activities, even though they are no longer active, can still negatively affect groundwater quality even today;
- results provide key information, which can be easily understood by stakeholders and decision makers and represent an extremely useful support for the improvement of environmental planning and groundwater management and protection strategies. Strategies could include: a) the progressive decommissioning of multi-aquifer wells, b) the relocation of wells in the deep aquifer that are located close to zones with low thickness of aquitard, c) more rigorous control on industrial and commercial activities in highly susceptible areas, d) site specific investigations in selected susceptible areas to check the eventual presence of residual DNAPL phases on the aquitard separating shallow and deep aquifers.

## Acknowledgements

We wish to acknowledge the Italian Ministry of Education (MIUR) that partially supported this work through the project “Dipartimenti di Eccellenza 2018-2022”.

## References

- Agterberg, F.P., Bonham-Carter, G.F., Cheng, Q., Wrights, D.F., 1993. Weights of evidence modelling and weighted logistic regression for mineral potential. In: Davis J.C., Herzfeld U.C. (Editors), *Computers in Geology-25 Years of Progress*, Oxford University Press, New York, NY, 13–32.
- Alberti, L., Azzellino, A., Colombo, L., Lombi, S., 2016a. Use of cluster analysis to identify tetrachloroethylene pollution hotspots for the transport numerical model implementation in urban functional area of Milan, Italy, in: *International Multidisciplinary Scientific GeoConference Surveying Geology and Mining Ecology Management, SGEM*. <https://doi.org/10.5593/SGEM2016/B11/S02.091>
- Alberti, L., Cantone, M., Colombo, L., Lombi, S., Piana, A., 2016b. Numerical modeling of regional groundwater flow in the Adda-Ticino Basin: Advances and new results. *Rendiconti Online Società Geologica Italiana* 41, 10–13. <https://doi.org/10.3301/ROL.2016.80>.
- Alberti, L., Colombo, L., Formentin, G., 2018. Null-space Monte Carlo particle tracking to assess groundwater PCE (Tetrachloroethene) diffuse pollution in north-eastern Milan functional urban area. *Sci. Total Environ.* 621, 326–339. <https://doi.org/10.1016/j.scitotenv.2017.11.253>.
- Aller L., Bennet T., Lehr J.H., Petty R.J., 1987. DRASTIC: a standardised system for evaluating groundwater pollution potential using hydrologic settings. US EPA Report, 600/2–87/035, “Robert S. Kerr” Environmental Research Laboratory, Ada, OK.
- Anderson, M.P., Woessner, W.W., 1992. *Applied groundwater modeling: simulation to flow and advective transport*, first ed., Academic Press, San Diego, U.S.A.
- Arthur, J.D., Wood, H.A.R., Baker, A.E., Cichon, J.R., Raines, G.L., 2007. Development and Implementation of a Bayesian-based Aquifer Vulnerability Assessment in Florida. *Natural Resources Research* 16 (2), 93–107. <https://doi.org/10.1007/s11053-007-9038-5>.
- Azzellino, A., Colombo, L., Lombi, S., Marchesi, V., Piana, A., Merri, A., Alberti, L., 2019. Groundwater diffuse pollution in functional urban areas: The need to define anthropogenic diffuse pollution background levels. *Sci. Total Environ.* 656, 1207–1222. <https://doi.org/10.1016/j.scitotenv.2018.11.416>.

- Beaujean, J., Lemieux, J.-M., Dassargues, A., Therrien, R., Brouyère, S., 2014. Physically Based Groundwater Vulnerability Assessment Using Sensitivity Analysis Methods. *Groundwater* 52, 864–874. <https://doi.org/10.1111/gwat.12132>.
- Berbenni, P., Cavallaro, A., Mori, B., 1993. The groundwater pollution in Lombardy (North Italy) caused by organo-halogenated compounds. *Ann. Ist. Sup. Sanità*, 29, 253–262.
- Beretta, G.P., Bianchi, M., 2004. In situ remediation of an Hexavalent Chromium contaminated site in Milan area (Italy) by soil flushing and geochemical fixation. *Geologia Tecnica e Ambientale*, 4.
- Bonham-Carter, G.F., 1994. *Geographic Information Systems for Geoscientists: modelling with GIS*. Pergamon Press, New York, U.S.A.
- Cavallaro, A., Corradi, C., Di Felice, G., Grassi, P., 1985. Underground water pollution in Milan and the province by industrial chlorinated-organic compounds. In: *Effects of land use on fresh waters*. Hellis Horwood Limited, Chichester, 68–84.
- Civita, M., 1994. Le Carte della vulnerabilità degli acquiferi all'inquinamento. *Teoria e Pratica. (Aquifers vulnerability maps to contamination. Theory and Practice)*, Pitagora Editrice, Bologna, pp. 325.
- Colombo, L., Alberti, L., Mazzon, P., Formentin, G., 2019. Transient Flow and Transport Modelling of an Historical CHC Source in North-West Milano. *Water* 11 (9), 1745. <https://doi.org/10.3390/w11091745>.
- Cortés, A., Puigserver, D., Carmona, J.M., Viladevall, M., 2011. Biological remediation approach involving soils and groundwaters polluted with chlorinated solvents in a Mediterranean context. In: *Recent Advances in Pharmaceutical Sciences*, Diego Muñoz-Torrero (Ed.), Transworld Research Network, India, pp. 223–246.
- Cowan, N., 2001. The magical number 4 in short-term memory: a reconsideration of mental storage capacity. *Behav. Brain Sci.* 24, 87–185. <https://doi.org/10.1017/S0140525X01003922>.
- Chung, C.F., Fabbri, A.G., 1999. Probabilistic Prediction Models for Landslide Hazard Mapping. *Photogramm. Eng. Remote Sens.* 65(12), 1389–1399.
- De Caro, M., Crosta, G.B., Frattini, P., 2017. Hydrogeochemical characterization and Natural Background Levels in urbanized areas: Milan Metropolitan area (Northern Italy). *J. Hydrol.* 547, 455–473. <https://doi.org/10.1016/j.jhydrol.2017.02.025>.
- De Luca, D.A., Destefanis, E., Forno, M.G., Lasagna, M., Masciocco, L., 2014. The genesis and the hydrogeological features of the Turin Po Plain fontanili, typical lowland springs in Northern Italy. *B. Eng. Geo. Environ.* 73 (2), 409–427. <https://doi.org/10.1007/s10064-013-0527-y>.

- Duke, C., Steele, J., 2010. Geology and lithic procurement in Upper Palaeolithic Europe: a weights-of-evidence based GIS model of lithic resource potential. *Journal of Archaeological Science* 37, 813–824. <https://doi.org/10.1016/j.jas.2009.11.011>.
- Eberts, S.M., Böhlke, J.K., Kauffman, L.J., Jurgens, B.C., 2012. Comparison of particle-tracking and lumped-parameter age-distribution models for evaluating vulnerability of production wells to contamination. *Hydrogeology Journal* 20, 263–282. <https://doi.org/10.1007/s10040-011-0810-6>.
- Eberts, S.M., Thomas, M.A., Jagucki, M.L., 2013, The quality of our Nation’s waters—Factors affecting public-supply-well vulnerability to contamination—Understanding observed water quality and anticipating future water quality: U.S. Geological Survey Circular 1385, 120 p.
- ERSAF - Ente Regionale per i Servizi all’Agricoltura e alle Foreste, 2018. DUSAF (Destinazione d’Uso dei Suoli Agricoli e Forestali) (*Land use database*). <http://www.cartografia.regione.lombardia.it/> (accessed 16 July 2019).
- ESRI - Environmental Systems Research Institute, 2010. ArcGIS Desktop 10, Redlands, CA.
- European Commission, 1998. Council Directive 98/83/EC of 3 November 1998 on the quality of water intended for human consumption (Drinking Water Directive). OJL 330, 5 December 1998, pp. 32-54.
- Filippini, M., 2017. Migration of chlorinated hydrocarbons in multilayer unconsolidated porous media: a case study from the Po Plain, Italy. *Acque Sotterranee - Italian Journal of Groundwater* 7 (4), 37–48. <https://doi.org/10.7343/as-2017-305>.
- Focazio, M.J., Reilly, T.E., Rupert, M.G., Helsel, D.R., 2002. Assessing Ground-Water Vulnerability to Contamination: Providing Scientifically Defensible Information for Decision Makers. U.S. Geological Survey Circular 1224. ISBN: 0-607-89025-8.
- Foster, S., 1987. Fundamental concepts in aquifer vulnerability, pollution risk and protection strategy. In: Duijvenbooden W van, and Waegeningh HG van (ed.), *Vulnerability of soil and groundwater to pollutants* 38, 69–86. Proceedings and Information, TNO Committee on Hydrological Research, The Hague.
- Foster, S., Hirata, R., Andreo, B., 2013. The aquifer pollution vulnerability concept: aid or impediment in promoting groundwater protection? *Hydrogeol. J.* 21, 1389–1392. <https://doi.org/10.1007/s10040-013-1019-7>.
- Gemitzi, A., Petalas, C., Tsihrintzis, V.A., Pissinaras, V., 2006. Assessment of groundwater vulnerability to pollution: a combination of GIS, fuzzy logic and decision making techniques. *Environmental Geology* 49, 653–673. <https://doi.org/10.1007/s00254-005-0104-1>.

- Giovanardi, A., 1979. Pollution by organic chloride compounds of the aquifers of the region of Milan. *Rivista Italiana d'Igiene* 39, 323–344.
- Gorla, M., 2001a. Acquiferi confinati profondi della Provincia di Milano: sviluppi delle conoscenze idrogeologiche e idrochimiche ai fini di un loro uso sostenibile. Parte 1 – Premessa e caratteristiche idrogeologiche. (*Deep confined aquifers within the Province of Milan: hydrogeological and hydrochemical evaluation for their sustainable use. Part 1<sup>st</sup> – Overview and hydrogeological features*). *Acque Sotterranee* 72, 9–24.
- Gorla, M., 2001b. Acquiferi confinati profondi della Provincia di Milano: sviluppi delle conoscenze idrogeologiche e idrochimiche ai fini di un loro uso sostenibile. Parte 2 – Caratteristiche geochemiche, inquinanti e conclusioni. (*Deep confined aquifers within the Province of Milan: hydrogeological and hydrochemical evaluation for their sustainable use. Part 2<sup>nd</sup> – Geochemical features, pollutants and conclusions*). *Acque Sotterranee* 73, 9–27.
- Gorla, M., Simonetti, R., Righetti, C., 2016. Basin-scale hydrogeological, geophysical, geochemical and isotopic characterization: an essential tool for building a Decision Support System for the sustainable management of alluvial aquifer systems within the provinces of Milan and Monza-Brianza (Northern Italy). *Acque Sotterranee - Italian Journal of Groundwater* 5 (3), 33–47. <https://doi.org/10.7343/as-2016-213>.
- Goovaerts, P., 1997. *Geostatistics for Natural Resources Evaluation (Applied Geostatistics)*. Oxford Univ. Press, New York, U.S.A.
- Izbicki, J.A., Ball, J.W., Bullen, T.D., Sutley, S.J., 2008. Chromium, chromium isotopes and selected trace elements, western Mojave Desert, USA. *Appl. Geochem.* 23 (5), 1325–1352. <https://doi.org/10.1016/j.apgeochem.2007.11.015>.
- Johnson, R.L., Clark, B.R., Landon, M.K., Kauffman, L.J., Eberts, S.M., 2011. Modeling the potential impact of seasonal and inactive multi-aquifer wells on contaminant movement to public water-supply wells. *J. Am. Water Resour. Assoc.* 47 (3), 588–596. <https://doi.org/10.1111/j.1752-1688.2011.00526.x>.
- Lee, S., Choi, J., Min, K., 2002. Landslide susceptibility analysis and verification using the Bayesian probability model. *Environmental Geology* 43 (1-2), 120–131. <https://doi.org/10.1007/s00254-002-0616-x>.
- Liggett, J.E., Talwar, S., 2009. Groundwater vulnerability assessments and integrated water resource management. *Streamline Watershed Management Bulletin*, 13(1), 18–29.
- Lynen, G., Zeman, P., Bakuname, C., Di Giulio, G., Mtui, P., Sanka, P., Jongejan, F., 2007. Cattle ticks of the genera *Rhipicephalus* and *Amblyomma* of economic importance in Tanzania: distribution assessed with

- GIS based on an extensive Weld survey. *Experimental and Applied Acarology* 43, 303–319. <https://doi.org/10.1007/s10493-007-9123-9>.
- Mair, A., El-Kadi, A.I., 2013. Logistic regression modeling to assess groundwater vulnerability to contamination in Hawaii, USA. *Journal of Contaminant Hydrology* 153, 1–23. <https://doi.org/10.1016/j.jconhyd.2013.07.004>.
- Masetti, M., Sterlacchini, S., Ballabio, C., Sorichetta, A., Poli, S., 2009. Influence of threshold value in the use of statistical methods for groundwater vulnerability assessment. *Sci. Total. Environ.* 407 (12), 3836–3846. <https://doi.org/10.1016/j.scitotenv.2009.01.055>.
- Mendoza, J. A., Barmen, G., 2006. Assessment of groundwater vulnerability in the Río Artiguas basin, Nicaragua. *Environmental Geology*, 50(4), 569–580. <https://doi.org/10.1007/s00254-006-0233-1>.
- Moran, M.J., Zogorski, J.S., Squillace, P.J., 2007. Chlorinated Solvents in Groundwater of the United States. *Environmental Science & Technology* 41(1), 74–81. <https://doi.org/10.1021/es061553y>.
- Nijenhuis, I., Schmidt, M., Pellegatti, E., Paramatti, E., Richnow, H.H., Gargini, A., 2013. A stable isotope approach for source apportionment of chlorinated ethene plumes at a complex multi-contamination events urban site. *J. Contam. Hydrol.* 153, 92–105. <https://doi.org/10.1016/j.jconhyd.2013.06.004>.
- Nolan, B.T., Hitt, K.J., 2006. Vulnerability of Shallow Groundwater and Drinking-Water Wells to Nitrate in the United States. *Environ. Sci. Technol.* 40, 7834–7840. <https://doi.org/10.1021/es060911u>.
- Palmer, C.D., Puls, R.W., 1994. Natural Attenuation of Hexavalent Chromium in Groundwater and Soils. EPA Groundwater Issue. EPA154015-941505
- Panno, S.V., Kelly, W.R., Martinsek, A.T., Hackley, K.C., 2006. Estimating background and threshold nitrate concentrations using probability graph. *Groundwater*, 44(5), 697–709. <https://doi.org/10.1111/j.1745-6584.2006.00240.x>.
- Pedretti, D., Masetti, M., Beretta, G.P., Vitiello, M., 2013. A Revised Conceptual Model to Reproduce the Distribution of Chlorinated Solvents in the Rho Aquifer (Italy). *Groundwater Monitoring & Remediation* 33 (3), 69–77. <https://doi.org/10.1111/gwmr.12017>.
- Poli, S., Sterlacchini, S., 2007. Landslide Representation Strategies in Susceptibility Studies using Weights-of-Evidence Modelling Technique. *Natural Resources Research* 16 (2), 121–134. <https://doi.org/10.1007/s11053-007-9043-8>.

- Pollicino, L.C., Masetti, M., Stevenazzi, S., Colombo, L., Alberti, L., 2019. Spatial Statistical Assessment of Groundwater PCE (Tetrachloroethylene) Diffuse Contamination in Urban Areas. *Water* 11 (6), 1211. <https://doi.org/10.3390/w11061211>.
- Pourghasemi, H.R., Moradi, H.R., Aghda, S.F., 2013. Landslide susceptibility mapping by binary logistic regression, analytical hierarchy process, and statistical index models and assessment of their performances. *Natural Hazards*, 69(1), 749–779. <https://doi.org/10.1007/s11069-013-0728-5>.
- Provincia di Milano, 1992. Indagini sulla Presenza di Composti Organo-Alogenati nelle Acque di Falda della Provincia di Milano. S.I.F. Provincia di Milano. Milano, Italy.
- Provincia di Milano, 2002. Fenomeni di contaminazione delle acque sotterranee nella provincia di Milano. Technical report, Provincia di Milano. Indagini per l'individuazione dei focolai-Titolo IV-L.R.62/85.
- Raines, G.L., 1999. Evaluation of Weights of Evidence to Predict Epithermal-Gold Deposits in the Great Basin of the Western United States. *Nat. Resour. Res.* 8, 257–276. <https://doi.org/10.1023/A:1021602316101>.
- Raines, G.L., Mihalasky, M.J., 2002. A Reconnaissance Method for Delineation of Tracts for Regional-Scale Mineral-Resource Assessment Based on Geologic-Map Data. *Natural Resources Research* 11, 241–248. <https://doi.org/10.1023/A:1021138910662>.
- Rajput, H., Goyal, R., Brighu, U., 2020. Modification and optimization of DRASTIC model for groundwater vulnerability and contamination risk assessment for Bhiwadi region of Rajasthan, India. *Environmental Earth Sciences* 79(6). <https://doi.org/10.1007/s12665-020-8874-z>.
- Regione Lombardia, Eni Divisione Agip, 2001. Geologia degli acquiferi Padani della Regione Lombardia [Geology of the Po Valley aquifers in Lombardy Region]. S.EL.CA., Florence, Italy.
- Repubblica Italiana, 2006. Norme in materia ambientale (*Environmental regulation*). D. Lgs. 3 Aprile 2006, n. 152, Roma.
- Rivett, M.O., Turner, R.J., Glibbery (née Murcott), P., Cuthbert, M.O., 2012. The legacy of chlorinated solvents in the Birmingham aquifer, UK: Observations spanning three decades and the challenge of future urban groundwater development. *J. Contam. Hydrol.* 140–141, 107–123. <https://doi.org/10.1016/j.jconhyd.2012.08.006>.
- Romero-Calcerrada, R., Luque, S., 2006. Habitat quality assessment using Weights-of-Evidence based GIS modelling: The case of *Picoides tridactylus* as species indicator of the biodiversity value of the Finnish forest. *Ecological Modelling*, 196, 62–76. <https://doi.org/10.1016/j.ecolmodel.2006.02.017>.

- Sacchi, E., Acutis, M., Bartoli, M., Brenna, S., Delconte, C.A., Laini, A., Pennisi, M., 2013. Origin and fate of nitrates in groundwater from the central Po plain: Insights from isotopic investigations. *Applied Geochemistry*, 34, 164–180. <https://doi.org/10.1016/j.apgeochem.2013.03.008>.
- Santi, P.M., McCray, J.E., Martens, J.L., 2006. Investigating cross-contamination of aquifers. *Hydrogeol. J.* 14, 51–68. <https://doi.org/10.1007/s10040-004-0403-8>.
- Sawatzky, D.L., Raines, G.L., Bonham-Carter, G.F., Looney, C.G., 2009. Spatial Data Modeller (SDM): ArcMAP 9.3 geoprocessing tools for spatial data modelling using weights of evidence, logistic regression, fuzzy logic and neural networks.
- Segre, M., 1987. Organic chlorine compounds pollution of Milan groundwater: two cases. *Acqua Aria*, Italy.
- Shrestha, S., Semkuyu, D. J., & Pandey, V. P., 2016. Assessment of groundwater vulnerability and risk to pollution in Kathmandu Valley, Nepal. *Science of The Total Environment*, 556, 23–35. <https://doi.org/10.1016/j.scitotenv.2016.03.021>.
- Sinclair, A.J., 1974. Selection of threshold values in geochemical data using probability graphs. *J. Geochem. Explor.* 3, 129–149.
- Sorichetta, A., Masetti, M., Ballabio, C., Sterlacchini, S., 2012. Aquifer nitrate vulnerability assessment using positive and negative weights of evidence methods, Milan, Italy. *Comput. Geosci.* 48, 199–210. <https://doi.org/10.1016/j.cageo.2012.05.021>.
- Sorichetta, A., Masetti, M., Ballabio, C., Sterlacchini, S., Beretta, G.P., 2011. Reliability of groundwater vulnerability maps obtained through statistical methods. *J. Environ. Manage.* 92, 1215–1224. <https://doi.org/10.1016/j.jenvman.2010.12.009>.
- Stevenazzi, S., Bonfanti, M., Masetti, M., Nghiem, S.V., Sorichetta, A., 2017. A versatile method for groundwater vulnerability projections in future scenarios. *J. Environ. Manage.* 187, 365–374. <https://doi.org/10.1016/j.jenvman.2016.10.057>.
- Stevenazzi, S., Masetti, M., Nghiem, S.V., Sorichetta, A., 2015. Groundwater vulnerability maps derived from a time-dependent method using satellite scatterometer data. *Hydrogeol. J.* 23, 631–647. <https://doi.org/10.1007/s10040-015-1236-3>.
- Stumpp, C., Żurek, A.J., Wachniew, P., Gargini, A., Gemitzi, A., Filippini, M., Witczak, Stanisław, W., 2016. A decision tree tool supporting the assessment of groundwater vulnerability. *Environ. Earth Sci.* 75(13), 1057. <https://doi.org/10.1007/s12665-016-5859-z>.

- Tesoriero, A.J., Voss, F.D., 1997. Predicting the Probability of Elevated Nitrate Concentrations in the Puget Sound Basin: Implications for Aquifer Susceptibility and Vulnerability. *Groundwater* 35, 1029–1039. <https://doi.org/10.1111/j.1745-6584.1997.tb00175.x>.
- Tiwari, A.K., Orioli, S., De Maio, M., 2019. Assessment of groundwater geochemistry and diffusion of hexavalent chromium contamination in an industrial town of Italy. *J. Contam. Hydrol.* 225, 103503. <https://doi.org/10.1016/j.jconhyd.2019.103503>.
- Uhan, J., Vižintin, G., Pezdič, J., 2011. Groundwater nitrate vulnerability assessment in alluvial aquifer using process-based models and weights-of-evidence method: Lower Savinja Valley case study (Slovenia). *Environ. Earth. Sci.* 64(1), 97–105. <https://doi.org/10.1007/s12665-010-0821-y>.
- UNPD - United Nations Population Division, 2018. World Urbanisation Prospects, the 2018 Revision: Key Facts. <https://esa.un.org/unpd/wup/Publications/Files/WUP2018-KeyFacts.pdf> (accessed 9 July 2019).
- Wachniew, P., Zurek, A.J., Stumpp, C., Gemitzi, A., Gargini, A., Filippini, M., Rozanski, K., Meeks, J., Kværner, J., Witczak, S., 2016. Toward operational methods for the assessment of intrinsic groundwater vulnerability: A review. *Critical Reviews in Environmental Science and Technology* 46, 827–884. <https://doi.org/10.1080/10643389.2016.1160816>.
- White, R., Rivett, M.O., Tellam, J.H., 2008. Paleo-roothole facilitated transport of aromatic hydrocarbons through a Holocene clay bed. *Environmental Science and Technology*, 42(19), 7118–7124. <https://doi.org/10.1021/es800797u>.
- Winkel, L., Berg, M., Amini, M., Hug, S.J., Annette Johnson, C., 2008. Predicting groundwater arsenic contamination in Southeast Asia from surface parameters. *Nature Geosci* 1, 536–542. <https://doi.org/10.1038/ngeo254>.
- WWAP - United Nations World Water Assessment Program, 2012. The United Nations World Water Development Report 4: Managing Water under Uncertainty and Risk. UNESCO, Paris.